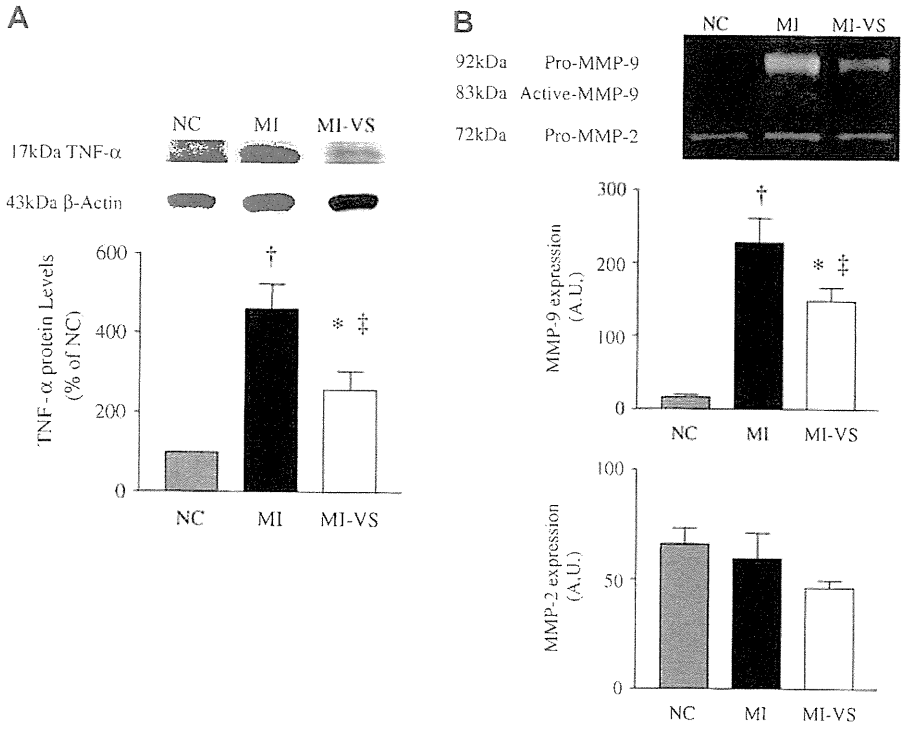

Fig. 2. Myocardial protein expressions of tumor necrosis factor-α (TNF-α) and matrix metalloproteinases (MMPs) in normal control rabbits (NC, n = 3), rabbits with reperfused myocardial infarction (MI) (n = 6), and MI rabbits treated with vagal nerve stimulation (MI-VS) rabbits (n = 6). (A) Representative Western blots of TNF-α (17 kDa) as well as corresponding β-actin bands (43 kDa) and band intensities normalized to NC values are shown. (B) Representative zymogram shows pro-MMP-9 band at 92 kDa and pro-MMP-2 band at 72 kDa. Note the faint 83 kDa band in MI hearts, which represents active MMP-9. Densitometric analysis of MMP-9 and MMP-2 contents expressed in integrated optical density (A.U.) relative to background. Data are means ± SEM. $^{*}P < .05$, $^{\dagger}P < .01$ versus NC. $^{\ddagger}P < .05$ versus MI.

blot analysis of other species of MMPs is summarized in Table 2. Myocardial protein levels of MMP-1 (50 kDa, pro-MMP-1) and MMP-7 (28 kDa, pro-MMP-7) decreased significantly to similar degrees in the MI and MI-VS groups compared to NC values. Myocardial protein level of MMP-8 (75 kDa, pro-MMP-8) increased significantly in the MI group compared with NC and MI-VS values (Table 2).

Table 2. Myocardial Protein Expression (Study 1)

	NC (n)	MI (n)	MI-VS (n)
IL-1β, % of NC	100 ± 6 (3)	79 ± 8 (6)	105 ± 25 (5)
IL-6, ng/g protein	52 ± 2 (3)	100 ± 7 (3) *	97 ± 13 (4)*
MMP-1, % of NC	100 ± 6 (3)	54 ± 8 (6) †	71 ± 12 (6)*
MMP-7, % of NC	100 ± 18 (3)	40 ± 10 (3) *	18 ± 2 (3)†
MMP-8, % of NC	100 ± 15 (3)	510 ± 82 (3) †	236 ± 65 (3)‡
TIMP-1, ng/g protein	39 ± 1 (3)	1394 ± 101 (6)†	1387 ± 164 (6)†
CRP, μg/g protein	13 ± 3 (3)	1926 ± 225 (6)†	1741 ± 114 (6)†

IL, interleukin; MMP, matrix metalloproteinase; TIMP, tissue inhibitor of metalloproteinase; CRP, C-reactive protein.

Data are means ± SEM. The number of hearts used for each experiment is given in parentheses.

$^{*}P < .05$.

$^{\dagger}P < .01$ versus NC.

$^{\ddagger}P < .05$ versus MI.

Myocardial level of TIMP-1 protein increased significantly to similar degrees in MI and MI-VS groups compared with NC values (Table 2).

Myocardial level of CRP increased significantly to similar degrees in the MI and MI-VS groups compared with NC values (Table 2).

Neutrophil Infiltration. No myocardial neutrophil infiltration was found in NC rabbits, whereas intense neutrophil infiltration into the infarcted myocardium was observed in MI rabbits (Fig. 3A). On the other hand, a significantly reduced neutrophil density in the infarcted myocardium was evident in MI-VS rabbits compared with MI animals (Fig. 3A, B). In accordance with neutrophil counts, myeloperoxidase activity in MI-VS rabbits was significantly reduced compared with MI animals (Fig. 3C).

Study 2: Chronic Phase after MI

Body Weight and Survival. Baseline body weights were comparable among the NC (2693 ± 184 g), MI (2530 ± 38 g), and MI-VS (2462 ± 24 g) groups. At 3 days after coronary reperfusion, body weights decreased to the same extent in both the MI (2325 ± 38 g) and MI-VS (2361 ± 53 g) groups. At 8 weeks after reperfusion, body weights increased to similar degrees in the MI (2843 ± 69 g) and

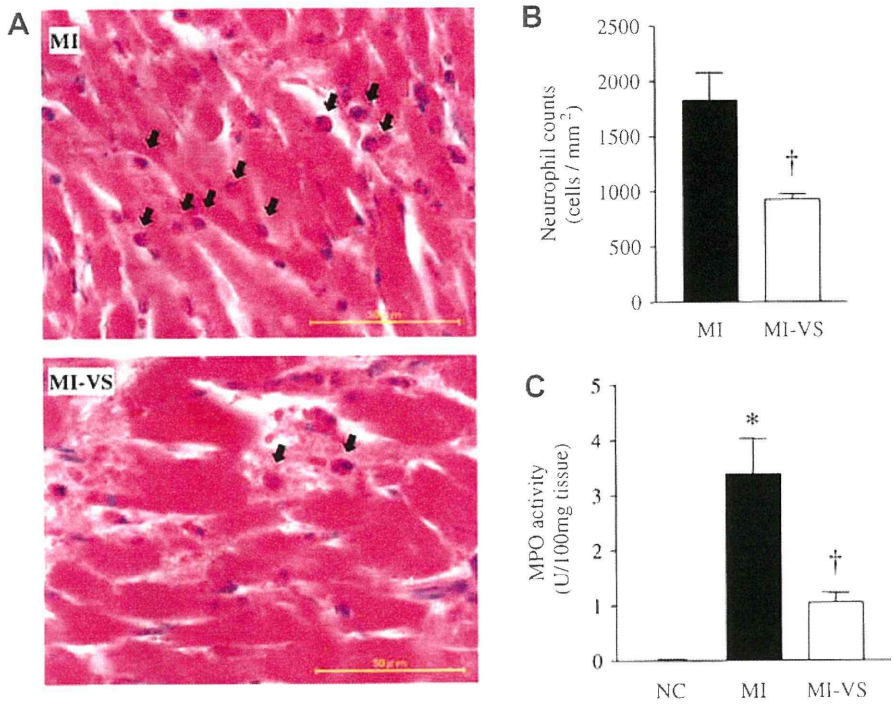

Fig. 3. (A) Photomicrographs of hematoxylin-eosin stained left ventricle cross-sections in infarcted regions obtained from rabbits with reperfused myocardial infarction (MI) and MI rabbits treated with vagal nerve stimulation (MI-VS) rabbits at 24 hours after coronary reperfusion. Arrows indicate infiltrating neutrophils. Bars = 50 μm. (B) Neutrophil counts of sections in infarct regions from MI (n = 6) and MI-VS (n = 6) rabbits. (C) Myocardial myeloperoxidase (MPO) activity in NC rabbits (n = 3), and in the infarct regions from MI (n = 4) and MI-VS (n = 4) rabbits. $^{*}P < .01$ versus NC, $^{\dagger}P < 0.01$ versus MI.

MI-VS (2899 ± 53 g) groups compared with the respective baseline values.

Five MI and four MI-VS rabbits died and the mortality rate up to 8 weeks after coronary reperfusion was comparable between the MI and MI-VS groups (31% versus 29%, P = NS). Of these deaths, 2 MI (13%) and 3 MI-VS (21%) rabbits died from arrhythmia at MI induction (P = NS).

Hemodynamics and LV Function. HR at 3 days after coronary reperfusion significantly increased in both the MI and MI-VS groups from their respective baseline values (Table 1). There were no significant differences in HR between the MI and MI-VS groups at baseline, after 30 minutes of coronary occlusion, and at 3 days after coronary reperfusion.

Baseline LV diameters and fractional shortening were similar in the MI and MI-VS groups (Table 3). At 3 days after coronary reperfusion, LV fractional shortening was reduced and LVESD was increased from baseline in both the MI and MI-VS groups to similar degrees. However, further deterioration of LV fractional shortening at 8 weeks after reperfusion observed in MI rabbits was prevented in MI-VS rabbits (Table 3). At 8 weeks after coronary reperfusion, MI-VS rabbits showed significantly smaller LVESD and LVEDD compared with MI rabbits. Data of invasive hemodynamic study are summarized in Table 4. Because 2 rabbits in the MI group with severely depressed LV function (LVEDD >20 mm, LV fractional shortening <14%) developed cardiac arrest during the induction of anesthesia, they were excluded from the invasive hemodynamic study. LV end-diastolic pressure was significantly increased in MI rabbits, which was significantly attenuated in MI-VS rabbits.

LV Passive Pressure-volume Relationship and LV Weight. Plots of ex vivo LV passive pressure-volume relationship are shown in Fig. 4A. A marked difference

Table 3. Changes in Echocardiographic Parameters with Time (Study 2)

	Baseline	3 Days	8 Weeks
LVESD, mm			
MI	7.8 ± 0.2	10.9 ± 0.2†	15.5 ± 0.6†,§
MI-VS	7.9 ± 0.4	9.8 ± 0.5*	11.4 ± 1.1$^{\dagger,\#}$
LVEDD, mm			
MI	13.0 ± 0.3	14.6 ± 0.3	19.2 ± 0.6†,§
MI-VS	12.8 ± 0.3	13.3 ± 0.5	15.5 ± 1.0$^{\dagger,\ddagger,\#}$
FS, %			
MI	39.9 ± 1.3	24.9 ± 1.5†	19.6 ± 1.6†,‡
MI-VS	38.6 ± 1.9	27.1 ± 1.2†	27.2 ± 2.6$^{\dagger,\|\|}$

3 d, 3 days after coronary reperfusion; 8 w, 8 weeks after coronary reperfusion; LVESD, left ventricular (LV) end-systolic diameter; LVEDD, LV end-diastolic diameter; FS, LV fractional shortening.

Data are means ± SEM.

n = 11 in MI group.

n = 10 in MI-VS group.

$^{*}P < .05$.

$^{\dagger}P < .01$ versus baseline.

$^{\ddagger}P < .05$.

$^{\S}P < .01$ versus 3 days.

$^{\|}P < .05$.

$^{\#}P < .01$ versus MI.

Table 4. Invasive Hemodynamic Parameters 8 Weeks after Coronary Reperfusion (Study 2)

	NC	MI	MI-VS
HR, beat/min	335 ± 14	320 ± 5	322 ± 5
MAP, mm Hg	110 ± 3	112 ± 3	112 ± 4
LV dP/dt_{max}, mm Hg/s	4622 ± 234	4546 ± 229	4770 ± 348
LV EDP, mm Hg	4 ± 1	16 ± 3*	7 ± 2†

NC, normal control; HR, heart rate; MAP, mean arterial pressure; LV dP/dt_{max}, the maximum first derivative of left ventricular pressure; LV EDP, left ventricular end-diastolic pressure.

Data are means ± SEM.

n = 7 in NC group, n = 9 in MI group, n = 10 in MI-VS group.

*P < .01 versus NC.

†P < .05 versus MI.

between NC and MI hearts is evident, whereas the average curve derived from MI-VS hearts is close to that of NC hearts. As shown in Fig. 4B, LV size, indexed by LVV_{10}, of MI-VS hearts was significantly smaller than that of MI hearts (P < .01) and reached values close to those of NC hearts. LV weight normalized by body weight increased significantly in both MI and MI-VS hearts compared with NC value (Fig. 4C), but was significantly lower in MI-VS hearts than in MI hearts (P < .01).

Histomorphologic Analysis of LV. The risk area sizes were comparable in MI and MI-VS hearts (47 ± 3% vs. 51 ± 5%, P = NS). A transverse LV section demonstrated a smaller LV cavity in the heart receiving VS (Fig. 5A). The LV infarct size was significantly reduced in MI-VS hearts (P < .05) compared with MI hearts as shown in Fig. 5B. Because the risk area sizes were comparable in MI and MI-VS hearts, the reduction of infarct size seen in MI-VS rabbits was due to the VS treatment, not insufficient ischemic insults. Wall thickness in LV septum (non-infarct region) was comparable in MI and MI-VS hearts, whereas LV infarct wall thickness was significantly greater in MI-VS hearts than in MI hearts. This resulted in higher thinning ratios in MI-VS hearts than in MI hearts (Fig. 5B). Myocyte hypertrophy in the septum was attenuated in MI-VS hearts as demonstrated by significantly reduced myocyte cross-sectional area compared with MI hearts. Collagen densities in viable myocardial tissue were similar in MI and MI-VS hearts (11 ± 1% versus 9 ± 0%, P = NS).

Plasma MMP. Relative MMP-9 level in plasma was comparable among NC (156 ± 19 A.U., n = 6), MI (147 ± 28 A.U., n = 7), and MI-VS (146 ± 22 A.U., n = 7) groups. Relative MMP-2 level in the MI-VS group (164 ± 20 A.U.) was significantly lower compared with those in the NC (226 ± 17 A.U.) and MI (230 ± 16 A.U.) groups (P < .05).

Subgroup Analysis of Effects of VS on LV Remodeling in Large MI. Because the progression of LV remodeling is problematic, especially in patients with large infarct

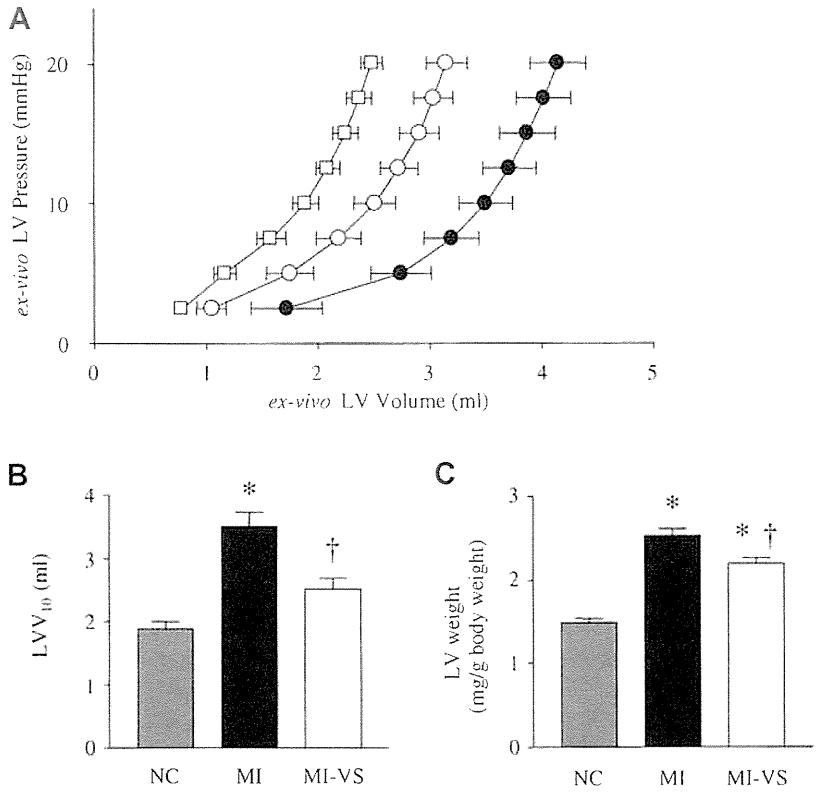

Fig. 4. Ex vivo left ventricular (LV) examinations of normal control (NC) (n = 7), reperfused myocardial infarction (MI) (n = 11), and MI rabbits treated with vagal nerve stimulation (MI-VS) (n = 10) hearts. (A) LV passive pressure-volume relationship in NC (□), MI (●), and MI-VS (○) hearts. (B) Ex vivo LV volume at LV pressure of 10 mm Hg (LVV_{10}). (C) LV weight normalized by body weight. *P < .01 versus NC. †P < .01 versus MI.

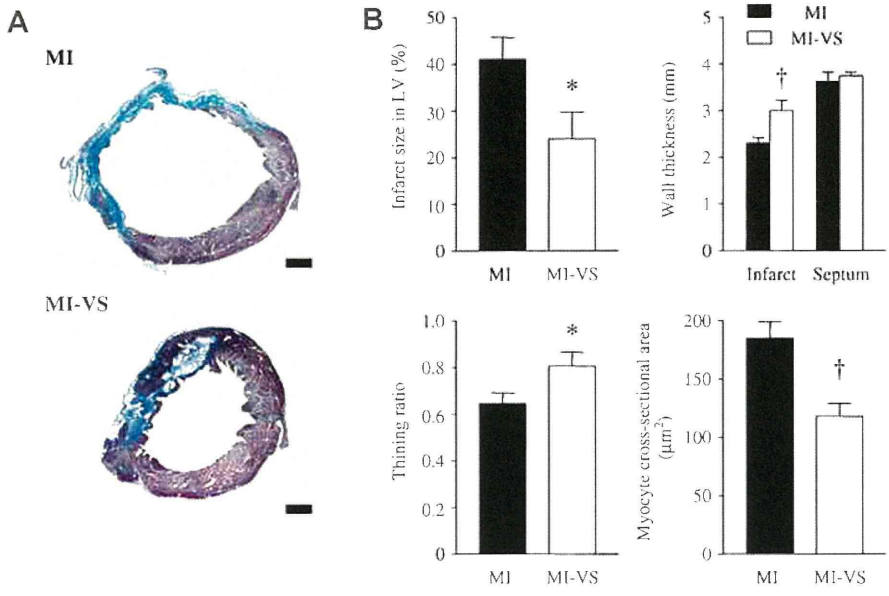

Fig. 5. (A) Transverse LV sections obtained from reperfused myocardial infarction (MI) and MI rabbits treated with vagal nerve stimulation (MI-VS) hearts 8 weeks post-MI. The sections were stained with Masson's trichrome. Blue stained area indicates scared infarct area. Bars = 3 mm. (B) Histomorphometric analyses of LVs in MI (n = 11) and MI-VS (n = 10) hearts. $^{*}P < .05$, $^{\dagger}P < .01$ versus MI.

size,[1] we evaluated the effects of VS on the parameters of LV remodeling (LV weight and LVEDD at 8 weeks after coronary reperfusion) in animals with large infarct size (>30% of LV, 8 MI. and 4 MI-VS rabbits). LV infarct size was comparable in MI and MI-VS hearts (49 ± 3% versus 44 ± 6%, P = NS). However, LV weight was significantly lower in MI-VS hearts than in MI hearts (2.2 ± 0.1 versus 2.6 ± 0.1 mg/g body weight, $P < .05$). There was a strong trend of reduction in LVEDD in MI-VS hearts compared with MI hearts, although the difference did not reach statistical significance (15.1 ± 2.0 versus 18.9 ± 0.8 mm, $P = .052$).

Discussion

The major new findings of the present study were as follows. In the acute inflammatory phase of reperfused MI, VS decreased TNF-α protein level and suppressed neutrophil infiltration in the infarcted myocardium. In the chronic phase of reperfused MI, VS markedly attenuated LV dysfunction and remodeling, even though VS was limited to a short period early after MI. Although several acute experimental studies examined the cardioprotective effects of VS in reperfused MI, they lacked detailed assessment of LV function and structure as done in this study.[5–7]

Cardioprotective Effects of VS and Cytokine Expressions

The beneficial effects of VS on reperfused MI are primarily attributable to the reduction of infarct size.[1,21] Several cardioprotective mechanisms of VS in ischemic myocardium have been reported previously. In a neutrophil-free isolated heart preparation, VS attenuated ischemia-reperfusion injury by protecting the myocytic mitochondria.[5] In a non-reperfused MI model, VS protected cardiomyocytes by upregulating hypoxia-inducible factor-1α pathway, and reduced infarct size.[22] Acetylcholine, the principal vagal neurotransmitter, mediated these direct protective effects on cardiomyocyte through the muscarinic acetylcholine receptor pathway.[5,22] These mechanisms may have contributed to the reduction of infarct size by VS in the present study. In addition, suppression of myocardial neutrophil infiltration in acute MI phase might also contribute to the reduction of infarct size by VS. Although reperfusion of the ischemic myocardium is necessary to salvage viable myocytes from eventual death, reperfusion also causes tissue damage.[9] Reperfusion injury in the acute phase of MI shares many characteristics with inflammatory reactions. Neutrophils feature prominently in this inflammatory reaction.[9] It is well known that in the reperfused ischemic myocardium, upregulated TNF-α accelerates the infiltration of neutrophils.[8,23] In this study, VS suppressed neutrophil infiltration into the infarcted myocardium possibly through inhibition of TNF-α expression, which might suppress the neutrophil-induced myocyte injury, thereby reducing the infarct size. Acetylcholine attenuates the release of TNF-α from macrophages through the nicotinic acetylcholine receptor pathway.[10,11] Cardiac mast cell is an important source of TNF-α in ischemic myocardium,[23] and expresses the nicotinic receptor.[24] In our model, VS might have directly reduced TNF-α expression on cardiac mast cells via the nicotinic acetylcholine receptor pathway.

Myocardial IL-1β protein content was not changed in our MI model. Previous experimental study also reported

similar results and suggested an insignificant role of IL-1β as an upstream inducer of post-reperfusion inflammatory reactions.[23] Myocardial IL-6 protein expression was not affected by VS in this study. Previous clinical study indicated that VS decreased plasma IL-6 concentration in patients with advanced heart failure, but the reduction was transient and noted only at 3 months after commencing VS.[4] Although the increase in plasma IL-6 has been associated with progression of LV contractile dysfunction in patients with heart failure, recent experimental research suggests that IL-6 expression in viable myocardium may play a pivotal role in cytoprotection.[25] Several biochemical and hemodynamic factors have been shown to regulate IL-6 expression after MI. IL-6 mRNA expression in mononuclear cells infiltrating the infarcted myocardium is upregulated by TNF-α.[23] Gwechenberger et al[16] have shown the reperfusion-dependent expression of IL-6 mRNA in cardiomyocytes in the viable border zone. Perfusion dependency of IL-6 expression was also observed in patients with reperfused MI, where plasma IL-6 concentration positively correlated with ischemic myocardial collateral flow.[26] In the present study, VS-induced TNF-α reduction might have decreased myocardial IL-6 expression. On the other hand, the beneficial effect of VS on myocardial perfusion[27] or the direct cardiomyocyte-protecting effect of VS[5] might have increased de novo synthesis of IL-6 in the jeopardized but viable myocardium. In VS, all these factors may operate simultaneously.

Myocardial CRP expression increased drastically after MI, which was not affected by VS in this study. After MI, CRP is produced from the liver partly as a response to stimulation by IL-6 released from the damaged heart.[28] Because we found that cardiac expression of IL-6 was similar in the MI and MI-VS groups, it is reasonable that myocardial CRP content was not different between the 2 groups in the present experiment. CRP-mediated complement activation in the myocardium was associated with increase in infarct size and LV remodeling after MI in several experimental and clinical studies,[28,29] although this association remains controversial.[30,31]

Our previous studies suggest that bradycardia plays a significant role in cardioprotection by VS.[3] However, the present results indicate that the cardioprotective effect of VS does not necessarily require strong bradycardia. Huston et al demonstrated that in a mouse model of sepsis, mild intensity of VS drastically reduces serum TNF-α without inducing bradycardia.[11] Furthermore, the cardioprotective effect of VS through protecting myocytic mitochondria is also independent of the degree of bradycardia.[5] Increasing VS intensity to attain strong bradycardia can cause unwanted side effects such as local pain in animals and also in patients.[3,4] Although the degree of bradycardia has been the primary parameter used in adjusting the intensity of VS,[4] additional parameters may be required for deciding the proper therapeutic strategy of VS in clinical application.

MMP Inhibition and LV Remodeling. Subgroup analysis of study 2 demonstrated that VS attenuated LV hypertrophy when comparing MI and MI-VS hearts with similarly large infarct size. This finding indicates that VS indeed confers an antiremodeling effect beyond that through reduction in infarct size. Reduction of MMP-9 activity in the infarcted myocardium early after MI may contribute to this antiremodeling effect of VS.[18,32–34] In addition to the loss of contractile cardiomyocytes, pathological degradation and reconstitution of extracellular matrix contribute to the progression of LV remodeling after MI, where MMP and TIMP play crucial roles. After MI, pharmacological MMP inhibition attenuated LV remodeling without affecting infarct size even if given for a short period.[18,33] Suppression of the infiltration of neutrophil, an important source of MMP-9 after myocardial ischemia reperfusion,[32] may be one reason of the reduction of MMP-9 contents by VS in infarct observed in this study. VS did not change the collagen content of the viable myocardium at 8 weeks after MI in spite of reduced MMP-9 expression early after MI. Several studies also reported that MMP inhibition improved LV remodeling without changing the collagen contents within the infarcts or in viable tissues after MI.[18,33] Lindsey et al demonstrated in a rabbit model of MI that inhibition of MMP activities attenuated LV dilatation and preserved the infarct wall thickness and the thinning ratio without changing the tissue collagen content.[33] Their findings are almost compatible to the present results. These observations suggest that a noncollagenolytic mechanism may also play a critical role in regulating LV remodeling. Plasma MMP-9 concentration measured 8 weeks after MI was not reduced in MI-VS rabbits compared with MI rabbits and controls. This indicates that the MMP-9 suppressive effect of VS delivered early after MI did not last long. This might be beneficial in terms of LV remodeling. A previous experimental study[34] demonstrated that MMP inhibition early after MI conferred beneficial effects on LV remodeling, but chronic prolonged MMP inhibition was associated with adverse effects on LV remodeling. MMP-8, a neutrophil collagenase, has been shown to increase in cardiac tissue after MI and relate to LV rupture in MI patients.[35] In this study, suppression of neutrophil infiltration is probably the primary reason for the reduction of myocardial MMP-8 contents by VS.

MMP-1 is mainly produced by cardiac fibroblasts. MMP-2 is mainly expressed in cardiomyocytes after ischemic injury.[35] MMP-7 is expressed in macrophages and cardiomyocytes after MI.[36] After reperfused MI, myocardial protein contents of MMP-1, -2, and -7 were not affected by VS. Taken together, VS appears to specifically affect neutrophil-associated MMPs.

Myocardial TIMP-1 protein level was not affected by VS in this study, which seems inconsistent with our previous finding.[12] TIMP-1 level increased drastically after 24 hours of coronary reperfusion in the present study (>1200 ng/g protein, compared with that observed after 3 hours of reperfusion in rabbits in our previous study (<500 ng/g protein).[12] On the other hand, the intensity of VS in this study was rather mild compared with that in the previous

study. These factors together may have obscured the TIMP-1–inducing property of VS in this study.

Clinical Implication

Early short-term VS strategy appears to be clinically feasible in patients with acute MI. Furthermore, this strategy may be both timely and sufficient based on the following evidence. First, upregulation of plasma and myocardial TNF-α as well as myocardial infiltration of neutrophils are mostly confined to within 3 days after MI.[15,37] Meanwhile, the anti-inflammatory effects of VS are long-lasting. In mice, only 30 seconds of VS significantly suppressed TNF-α activation in response to lipopolysaccharide challenge even at 48 hours after VS.[11] Second, pharmacological inhibition of MMP activity for 48 hours after MI preserves the original extracellular matrix, thereby lessens LV remodeling.[18]

Although the present findings suggest clinically useful strategy of VS, several issues remain to be solved before VS can be considered for clinical application in patients with MI. First, it is unclear whether VS is able to provide additional therapeutic benefits to current pharmacological treatments such as renin-angiotensin-aldosterone inhibition or β-blockade, the efficacy of which has been well established in patients with MI.[38] Second, it is unclear whether VS started after reperfusion is also capable of attenuating LV remodeling after MI. Although we started VS during coronary occlusion in this study, initiating VS after coronary reperfusion may simulate a more clinically relevant situation, because prompt reperfusion of occluded coronary artery is given the utmost priority in the management of patients with acute MI. Further studies to solve these problems are clearly required.

VS did not afford any survival benefit in this study, which is inconsistent with previous findings that VS improves acute[7] or chronic[3] survival in rats after MI by preventing malignant arrhythmia and heart failure. However, the mortality rate in MI rats was ~60% within the first 24 hours in the previous study,[3] which is undoubtedly higher than that seen in MI rabbits of this study (~30%). Low mortality rate in MI rabbits may have masked the impact of VS on survival in this study.

Limitation

We focused on the antiremodeling effects of VS but did not include a detailed mechanistic investigation into how VS reduces LV infarct size. Inflammatory responses to MI play a significant role in determining the infarct size.[9] On the other hand, the infarct size, which reflects the degree of myocardial necrosis, is also one of the determinants of post-MI inflammatory reactions. Therefore, direct cardiomyocyte protection of VS possibly through the muscarinic acetylcholine pathway and the anti-inflammatory effect possibly through the nicotinic pathway may have contributed synergistically to the infarct size-reducing effect of VS. Selective inhibition of the muscarinic and nicotinic pathway by atropine and methyllycaconitine,[39] respectively, may allow elucidation of how these different mechanisms contribute to the beneficial effects of VS in a reperfused MI model. Further studies on these issues are clearly required.

Acute surgical trauma associated with open-chest preparation may have exaggerated the expression of CRP and TNF-α in MI and MI-VS rabbits in this study. For a more rational comparison of acute inflammatory reactions among NC, MI, and MI-VS animals, use of sham-operated rabbits as NC would be more appropriate. Closed-chest animal models of myocardial ischemia-reperfusion[40] may be an alternative to eliminate acute surgical trauma and allow assessment of inflammation strictly from myocardial injury. In this study, MI and MI-VS rabbits underwent identical surgical preparation. Therefore, it is fair to say that the difference in TNF-α expression in infarcts between the MI and MI-VS groups was valid in the present study.

In conclusion, early short-term VS attenuated cardiac dysfunction and myocardial structural remodeling in a rabbit model of reperfused MI. The beneficial effects of VS were associated with suppression of excessive TNF-α activation and myocardial infiltrations of neutrophils.

Acknowledgments

We thank Dr. Takeshi Aiba for his helpful comments on this manuscript.

Disclosures

Supported by Grant-in-Aid for Scientific Research from the Ministry of Education, Culture, Sports, Science and Technology (C-20500404 to K.U.), by a research grant from Nakatani Foundation of Electronic Measuring Technology Advancement (to K.U.), and by Health and Labour Sciences Research Grants from the Ministry of Health, Labour and Welfare of Japan (H19-nano-ippan-009 to M.S.).

References

1. Bolognese L, Cerisano G. Early predictors of left ventricular remodeling after acute myocardial infarction. Am Heart J 1999;138:S79–83.
2. Ezekowitz JA, Kaul P, Bakal JA, Armstrong PW, Welsh RC, McAlister FA. Declining in-hospital mortality and increasing heart failure incidence in elderly patients with first myocardial infarction. J Am Coll Cardiol 2009;53:13–20.
3. Li M, Zheng C, Sato T, Kawada T, Sugimachi M, Sunagawa K. Vagal nerve stimulation markedly improves long-term survival after chronic heart failure in rats. Circulation 2004;109:120–4.
4. Schwartz PJ, De Ferrari GM, Sanzo A, Landolina M, Rordorf R, Raineri C, et al. Long term vagal stimulation in patients with advanced heart failure: first experience in man. Eur J Heart Fail 2008;10:884–91.
5. Katare RG, Ando M, Kakinuma Y, Arikawa M, Handa T, Yamasaki F, et al. Vagal nerve stimulation prevents reperfusion injury through inhibition of opening of mitochondrial permeability transition pore independent of the bradycardiac effect. J Thorac Cardiovasc Surg 2009; 137:223–31.

6. Kawada T, Yamazaki T, Akiyama T, Kitagawa H, Shimizu S, Mizuno M, et al. Vagal stimulation suppresses ischemia-induced myocardial interstitial myoglobin release. Life Sci 2008;83:490–5.
7. Mioni C, Bazzani C, Giuliani D, Altavilla D, Leone S, Ferrari A, et al. Activation of an efferent cholinergic pathway produces strong protection against myocardial ischemia/reperfusion injury in rats. Crit Care Med 2005;33:2621–8.
8. Sun M, Dawood F, Wen WH, Chen M, Dixon I, Kirshenbaum LA, et al. Excessive tumor necrosis factor activation after infarction contributes to susceptibility of myocardial rupture and left ventricular dysfunction. Circulation 2004;110:3221–8.
9. Vinten-Johansen J. Involvement of neutrophils in the pathogenesis of lethal myocardial reperfusion injury. Cardiovasc Res 2004;61: 481–97.
10. Borovikova LV, Ivanova S, Zhang M, Yang H, Botchkina GI, Watkins LR, et al. Vagus nerve stimulation attenuates the systemic inflammatory response to endotoxin. Nature 2000;405:458–62.
11. Huston JM, Gallowitsch-Puerta M, Ochani M, Ochani K, Yuan R, Rosas-Ballina M, et al. Transcutaneous vagus nerve stimulation reduces serum high mobility group box 1 levels and improves survival in murine sepsis. Crit Care Med 2007;35:2762–8.
12. Uemura K, Li M, Tsutsumi T, Yamazaki T, Kawada T, Kamiya A, et al. Efferent vagal nerve stimulation induces tissue inhibitor of metalloproteinase-1 in myocardial ischemia-reperfusion injury in rabbit. Am J Physiol Heart Circ Physiol 2007;293:H2254–61.
13. LaCroix C, Freeling J, Giles A, Wess J, Li YF. Deficiency of M2 muscarinic acetylcholine receptors increases susceptibility of ventricular function to chronic adrenergic stress. Am J Physiol Heart Circ Physiol 2008;294:H810–20.
14. Hasdemir C, Scherlag BJ, Yamanashi WS, Lazzara R, Jackman WM. Endovascular stimulation of autonomic neural elements in the superior vena cava using a flexible loop catheter. Jpn Heart J 2003;44: 417–27.
15. Dewald O, Ren G, Duerr GD, Zoerlein M, Klemm C, Gersch C, et al. Of mice and dogs: species-specific differences in the inflammatory response following myocardial infarction. Am J Pathol 2004;164:665–77.
16. Gwechenberger M, Mendoza LH, Youker KA, Frangogiannis NG, Smith CW, Michael LH, et al. Cardiac myocytes produce interleukin-6 in culture and in viable border zone of reperfused infarctions. Circulation 1999;99:546–51.
17. Klotz S, Foronjy RF, Dickstein ML, Gu A, Garrelds IM, Danser AH, et al. Mechanical unloading during left ventricular assist device support increases left ventricular collagen cross-linking and myocardial stiffness. Circulation 2005;112:364–74.
18. Villarreal FJ, Griffin M, Omens J, Dillmann W, Nguyen J, Covell J. Early short-term treatment with doxycycline modulates postinfarction left ventricular remodeling. Circulation 2003;108:1487–92.
19. Newman KM, Ogata Y, Malon AM, Irizarry E, Gandhi RH, Nagase H, et al. Identification of matrix metalloproteinases 3 (stromelysin-1) and 9 (gelatinase B) in abdominal aortic aneurysm. Arterioscler Thromb 1994;14:1315–20.
20. Ernens I, Rouy D, Velot E, Devaux Y, Wagner DR. Adenosine inhibits matrix metalloproteinase-9 secretion by neutrophils: implication of A2a receptor and cAMP/PKA/Ca2+ pathway. Circ Res 2006;99: 590–7.
21. Ørn S, Manhenke C, Anand IS, Squire I, Nagel E, Edvardsen T, et al. Effect of left ventricular scar size, location, and transmurality on left ventricular remodeling with healed myocardial infarction. Am J Cardiol 2007;99:1109–14.
22. Kakinuma Y, Ando M, Kuwabara M, Katare RG, Okudela K, Kobayashi M, et al. Acetylcholine from vagal stimulation protects cardiomyocytes against ischemia and hypoxia involving additive nonhypoxic induction of HIF-1alpha. FEBS Lett 2005;579:2111–8.
23. Frangogiannis NG, Lindsey ML, Michael LH, Youker KA, Bressler RB, Mendoza LH, et al. Resident cardiac mast cells degranulate and release preformed TNF-alpha, initiating the cytokine cascade in experimental canine myocardial ischemia/reperfusion. Circulation 1998;98:699–710.
24. Kindt F, Wiegand S, Niemeier V, Kupfer J, Löser C, Nilles M, et al. Reduced expression of nicotinic alpha subunits 3, 7, 9 and 10 in lesional and nonlesional atopic dermatitis skin but enhanced expression of alpha subunits 3 and 5 in mast cells. Br J Dermatol 2008;159: 847–57.
25. Smart N, Mojet MH, Latchman DS, Marber MS, Duchen MR, Heads RJ. IL-6 induces PI 3-kinase and nitric oxide-dependent protection and preserves mitochondrial function in cardiomyocytes. Cardiovasc Res 2006;69:164–77.
26. Rakhit RD, Seiler C, Wustmann K, Zbinden S, Windecker S, Meier B, et al. Tumour necrosis factor-alpha and interleukin-6 release during primary percutaneous coronary intervention for acute myocardial infarction is related to coronary collateral flow. Coron Artery Dis 2005;16:147–52.
27. Buck JD, Warltier DC, Hardman HF, Gross GJ. Effects of sotalol and vagal stimulation on ischemic myocardial blood flow distribution in the canine heart. J Pharmacol Exp Ther 1981;216:347–51.
28. Ørn S, Manhenke C, Ueland T, Damås JK, Mollnes TE, Edvardsen T, et al. C-reactive protein, infarct size, microvascular obstruction, and left-ventricular remodelling following acute myocardial infarction. Eur Heart J 2009;30:1180–6.
29. Nijmeijer R, Lagrand WK, Lubbers YT, Visser CA, Meijer CJ, Niessen HW, et al. C-reactive protein activates complement in infarcted human myocardium. Am J Pathol 2003;163:269–75.
30. Sukhija R, Fahdi I, Garza L, Fink L, Scott M, Aude W, et al. Inflammatory markers, angiographic severity of coronary artery disease, and patient outcome. Am J Cardiol 2007;99:879–84.
31. Blankenberg S, McQueen MJ, Smieja M, Pogue J, Balion C, Lonn E, et al. Comparative impact of multiple biomarkers and N-Terminal pro-brain natriuretic peptide in the context of conventional risk factors for the prediction of recurrent cardiovascular events in the Heart Outcomes Prevention Evaluation (HOPE) Study. Circulation 2006;114: 201–8.
32. Kelly D, Cockerill G, Ng LL, Thompson M, Khan S, Samani NJ, et al. Plasma matrix metalloproteinase-9 and left ventricular remodelling after acute myocardial infarction in man: a prospective cohort study. Eur Heart J 2007;28:711–8.
33. Lindsey ML, Gannon J, Aikawa M, Schoen FJ, Rabkin E, Lopresti-Morrow L, et al. Selective matrix metalloproteinase inhibition reduces left ventricular remodeling but does not inhibit angiogenesis after myocardial infarction. Circulation 2002;105:753–8.
34. Spinale FG, Escobar GP, Hendrick JW, Clark LL, Camens SS, Mingoia JP, et al. Chronic matrix metalloproteinase inhibition following myocardial infarction in mice: differential effects on short and long-term survival. J Pharmacol Exp Ther 2006;318:966–73.
35. van den Borne SW, Cleutjens JP, Hanemaaijer R, Creemers EE, Smits JF, Daemen MJ, et al. Increased matrix metalloproteinase-8 and -9 activity in patients with infarct rupture after myocardial infarction. Cardiovasc Pathol 2009;18:37–43.
36. Lindsey ML, Escobar GP, Mukherjee R, Goshorn DK, Sheats NJ, Bruce JA, et al. Matrix metalloproteinase-7 affects connexin-43 levels, electrical conduction, and survival after myocardial infarction. Circulation 2006;113:2919–28.
37. Li D, Zhao L, Liu M, Du X, Ding W, Zhang J, et al. Kinetics of tumor necrosis factor alpha in plasma and the cardioprotective effect of a monoclonal antibody to tumor necrosis factor alpha in acute myocardial infarction. Am Heart J 1999;137:1145–52.
38. Landmesser U, Wollert KC, Drexler H. Potential novel pharmacological therapies for myocardial remodelling. Cardiovasc Res 2009;81: 519–27.
39. Liu C, Shen FM, Le YY, Kong Y, Liu X, Cai GJ, Chen AF, Su DF. Antishock effect of anisodamine involves a novel pathway for activating alpha7 nicotinic acetylcholine receptor. Crit Care Med 2009;37: 634–41.
40. Nossuli TO, Lakshminarayanan V, Baumgarten G, Taffet GE, Ballantyne CM, Michael LH, et al. A chronic mouse model of myocardial ischemia-reperfusion: essential in cytokine studies. Am J Physiol Heart Circ Physiol 2000;278:H1049–55.

J Physiol Sci (2010) 60:407–413
DOI 10.1007/s12576-010-0109-8

ORIGINAL PAPER

Both skeletonized and pedicled internal thoracic arteries supply adequate graft flow after coronary artery bypass grafting even during intense sympathoexcitation

Dai Une · Shuji Shimizu · Atsunori Kamiya · Toru Kawada · Toshiaki Shishido · Masaru Sugimachi

Received: 21 February 2010 / Accepted: 15 August 2010 / Published online: 14 September 2010

Abstract The internal thoracic artery (ITA) is harvested by either the pedicled or the skeletonized technique in coronary artery bypass grafting (CABG), with no clear advantage of one technique over the other. We compared graft flow between the pedicled and skeletonized ITA grafts while varying myocardial oxygen demand. CABG was performed to the left anterior descending artery in five anesthetized dogs using a pedicled ITA graft and the graft was subsequently skeletonized. Graft flow was measured during stepwise electrical stimulation of the stellate ganglion. The baseline graft flow before sympathetic stimulation was higher in skeletonized (27.8 ± 1.9 ml/min) than that in pedicled ITA grafts (22.6 ± 2.7 ml/min) ($P < 0.05$). In both ITA grafts, however, graft flow increased to a similar level during sympathetic stimulation that doubled the double product, correlating with the double product. Based on these results, we conclude that metabolic demand can override the potential difference in sympathetic vasoconstriction in both pedicled and skeletonized ITA grafts.

Keywords Coronary artery bypass grafting · Graft flow · Internal thoracic artery · Pedicled · Skeletonized · Sympathetic activation

D. Une · S. Shimizu (✉) · A. Kamiya · T. Kawada · T. Shishido · M. Sugimachi
Department of Cardiovascular Dynamics, National Cerebral and Cardiovascular Center Research Institute, 5-7-1 Fujishiro-dai, Suita, Osaka 565-8565, Japan
e-mail: shujismz@ri.ncvc.go.jp

S. Shimizu
Japan Association for the Advancement of Medical Equipment, Tokyo, Japan

Introduction

The internal thoracic artery (ITA) is the gold standard conduit for coronary artery bypass grafting (CABG) because of its long-term patency [1]. The ITA is harvested by either the pedicled or the skeletonized technique, and which of these two techniques is the better option has been the subject of an extended debate—with as yet no clear conclusion being drawn. Although some human studies [2–4] have demonstrated higher free (pre-anastomosis) flow through skeletonized grafts (with or without topical papaverine), suggesting that the loss of sympathetic nerve-mediated graft vasoconstriction confers an advantage, perfusion pressure was not controlled in these studies. In one study [5] in which the perfusion pressure was controlled, free flow even tended to be lower in skeletonized grafts prior to the administration of intravenous papaverine. Onorati et al. [6] found that graft flows were comparable between the two techniques in the absence of intraluminal papaverine, while Takami and Ina [7], in a comparison of the flow through the anastomosed graft, found that flow was higher through the skeletonized graft.

Flow in the anastomosed graft is likely to be largely dependent on myocardial oxygen demand, suggesting the importance of comparing the flow between the pedicled and skeletonized ITA grafts under varying conditions of myocardial oxygen demand. If the skeletonization procedure were to result in an increased flow capacity, surgeons may be able to perform additional anastomoses to other vessels using the skeletonized ITA, thereby making the skeletonized ITA procedure even more advantageous. If the skeletonization procedure were not able to increase flow capacity, the skeletonized ITA would not be recommended for additional use due to a higher flow reserve. We hypothesized that the skeletonized ITA would have larger

flow capacity due to the loss of sympathetic nerve-mediated graft vasoconstriction.

Materials and methods

Animal preparation

Animal care was provided in accordance with the *Guiding Principles for the Care and Use of Animals in the Field of Physiological Sciences* approved by the Physiological Society of Japan. All protocols were approved by the Animal Subject Committee of the National Cerebral and Cardiovascular Center. Five adult mongrel dogs (weighing 24–35 kg) were anesthetized with intravenous pentobarbital sodium (25 mg/kg) and intubated endotracheally for artificial ventilation with isoflurane and 100% O_2. After a median sternotomy, the heart was suspended in a pericardial cradle. To measure systemic arterial pressure, we placed a fluid-filled catheter in the left subclavian artery via the left brachial artery and connected it to a pressure transducer (DX-200; Nihon Kohden, Tokyo, Japan). The junction of the inferior vena cava and the right atrium was taken as the reference point for zero pressure. An ultrasonic flowmeter (20A594; Transonic Systems, Itaca, NY) was placed around the ascending aorta to measure cardiac output. Electrocardiography leads were also placed for the monitoring electrocardiogram. A catheter was inserted into the femoral vein for fluid replacement (1 ml/kg/h of Ringer's solution). All protocols were performed under open chest conditions.

Pedicled ITA grafting

The left internal thoracic artery (LITA), together with the surrounding veins, muscle, and fascia, was harvested as a pedicled graft using electrocautery. The LITA was harvested from the bifurcation of the musculo-phrenic and superior epigastric arteries up to the upper margin of the first rib or higher. All intercostal branches of the LITA were ligated. After systemic heparinization, the LITA was clamped, and the distal end of the LITA was cut and anastomosed to the left anterior descending artery (LAD). The same surgeon (D.U.) performed the LITA–LAD anastomosis without cardiopulmonary bypass. The heart and the LAD were stabilized using a compression-type mechanical stabilizer (Mini-CABG system; United States Surgical Corporation, Norwalk, CT). A shunt tube was inserted into the LAD to prevent myocardial ischemia during anastomosis. The anastomosis was placed in the mid-LAD [8]. The anastomosis was created using a continuous 7-0 polypropylene suture. The proximal LAD was first ligated after the LITA–LAD anastomosis, and then the LITA was declamped. An angiography was performed after the anastomosis to confirm the absence of stenosis or spasm in the LITA–LAD anastomosis. The LITA graft was sprayed with dilute papaverine (4 mg/ml) to prevent spasm. An ultrasonic flowmeter (2.5S261; Transonic Systems) was placed around the LITA just proximal to the anastomosis. The left stellate ganglion was carefully exposed through a median sternotomy, and a pair of platinum electrodes was attached to it without decentralization. The nerve and electrodes were covered with a mixture of silicone gel (Kwik-Sil; World Precision Instrument, Sarasota, FL). Protocol 1, described below, was carried out following the pedicled LITA grafting.

Skeletonized ITA grafting

Following the completion of protocol 1, the tissue surrounding the graft (including fascia and lymphatics) was stripped up to the most proximal part of the LITA graft in order to skeletonize the LITA graft. The side branches of the LITA were ligated. Fat tissue around the graft was removed as completely as possible based on macroscopic inspection. The adventitia was left as the outermost layer of the graft. The graft was not touched directly with forceps. The graft was sprayed with dilute papaverine (4 mg/ml). After skeletonizing the LITA graft, protocol 2 followed.

Experimental protocols

Since skeletonization always followed pedicled harvesting, protocol 1 (pedicled LITA graft flow measurement) was performed before protocol 2 (skeletonized LITA graft flow measurement) in all dogs. The stimulation of the left sympathetic stellate ganglion for adjusting the voltage amplitude was performed at least 30 min before protocol 1 was initiated.

Protocol 1

The left sympathetic stellate ganglion was electrically stimulated at least 30 min after the completion of the experimental preparation of the pedicled LITA grafts. The frequency of stimulation was increased stepwise from 0 to 10 Hz with increments of 2 Hz. Each step was maintained for 60 s. The pulse duration of the stimulus was set at 5 ms. The voltage amplitude of stimulation (2–5 V) was adjusted in each animal to yield an increase in arterial pressure of approximately 30 mmHg with 10 Hz stimulation. Graft flow, arterial pressure, and cardiac output were recorded for 7 min, which included a 2-min baseline and 5 min of stimulation. These data were sampled at 200 Hz using a 12-bit analog-to-digital converter [AD12-16U(PCI)E;

CONTEC, Osaka, Japan] and stored on the hard disk of a dedicated laboratory computer system.

Protocol 2

At least 30 min after the completion of the experimental preparation of the skeletonized LITA grafts, the left sympathetic stellate ganglion was electrically stimulated in a similar fashion to protocol 1, while all variables were recorded and stored.

Data analysis

Heart rate was calculated from the arterial pressure waveform. Myocardial oxygen demand was estimated as double product (pressure–rate product) and calculated as the product of systolic arterial pressure and heart rate [9]. All variables were averaged during the last 20 s of each electrical stimulation level.

Statistical analysis

All data are presented as the mean ± standard error (SE). In each protocol, one-way repeated measures analysis of variance (ANOVA) followed by Dunnett's test was used to compare variables at each stimulation against the baseline value. The paired t test was used to compare variables between pedicled and skeletonized LITA grafts at each stimulation level. Linear regression analysis was used to examine the relationship between the double product and graft flow. Differences were considered to be significant at a threshold of $P < 0.05$.

Results

Prior to sympathetic stimulation, baseline graft flow (under spontaneous sympathetic outflow) was greater in skeletonized ITA than pedicled ITA (Table 1). Other hemodynamic parameters, including heart rate, cardiac output, mean arterial pressure, and double product, did not differ significantly regardless of harvesting technique.

Table 1 Hemodynamic parameters and graft flow before stimulation

Hemodynamic parameters	Pedicled	Skeletonized	P value
Heart rate (beats/min)	104 ± 8	106 ± 8	NS
Mean arterial pressure (mmHg)	94 ± 7	93 ± 7	NS
Cardiac output (ml/min/kg)	83 ± 17	74 ± 9	NS
Double product (mmHg beats/min)	11368 ± 834	11346 ± 621	NS
Graft flow before stimulation (ml/min)	22.6 ± 2.7	27.8 ± 1.9	<0.05

Values are given as the mean ± standard error (SE)

NS Not significant

Graft flow patterns at baseline and under sympathetic stimulation are shown in Fig. 1a. Sympathetic stimulation increased graft flow ($P < 0.05$) similarly in skeletonized and pedicled ITA grafts, and maximal flow was comparable to each other at 10-Hz stimulation [nonsignificant (NS) difference] (Fig. 1b). Increases in systemic arterial pressure and heart rate did not differ significantly between the two techniques (Fig. 2), and increases in myocardial oxygen demand in response to sympathetic stimulation, as estimated by double product, were likewise similar.

Graft flow (y) correlated well with the double product (x) in both pedicled ($y = 2.6 \times 10^{-3}x - 8.4$, $R^2 = 0.73$) and skeletonized ITA ($y = 2.3 \times 10^{-3}x - 0.7$, $R^2 = 0.69$). The slope and y-intercept did not differ statistically between the two techniques (Fig. 3).

Discussion

The choice of either skeletonized or pedicled ITA grafts for CABG may be an important decision from both the technical and clinical viewpoints; however, clear evidence demonstrating the advantage of either method over the other is not yet available. In this study, we have shown that graft flow increased to a similar level during maximal sympathetic stimulation in both pedicled and skeletonized ITA grafts. These results do not support our hypothesis that the skeletonized ITA would provide larger flow capacity and indicate that coronary vasodilatation in response to increased myocardial oxygen demand is a stronger determinant of graft flow than any possible increase in the vascular resistance of ITA itself. Our study also demonstrates that both skeletonized and pedicled ITAs were able to supply adequate graft flow after CABG even during intense sympathoexcitation.

There are several possible explanations for the difference in graft flow under baseline conditions. First, a loss of sympathetic innervation in the skeletonized graft may have dilated the ITA relative to the pedicled graft under baseline conditions. In support of this explanation, Takami et al. [7] reported that the diameter of the ITA just proximal to the anastomosis is significantly larger in the skeletonized ITA than that in the pedicled ITA. Dönmez et al. [10] reported that the diameter of ITA becomes statically larger by the stellate ganglion blockade. In a preliminary study, we observed that electrical stimulation of the stellate ganglion decreased ITA flow before harvest. Therefore, vasoconstriction may occur in the pedicled ITA during sympathetic stimulation. However, in this study we did not perform simultaneous measurements of the graft flow and diameter

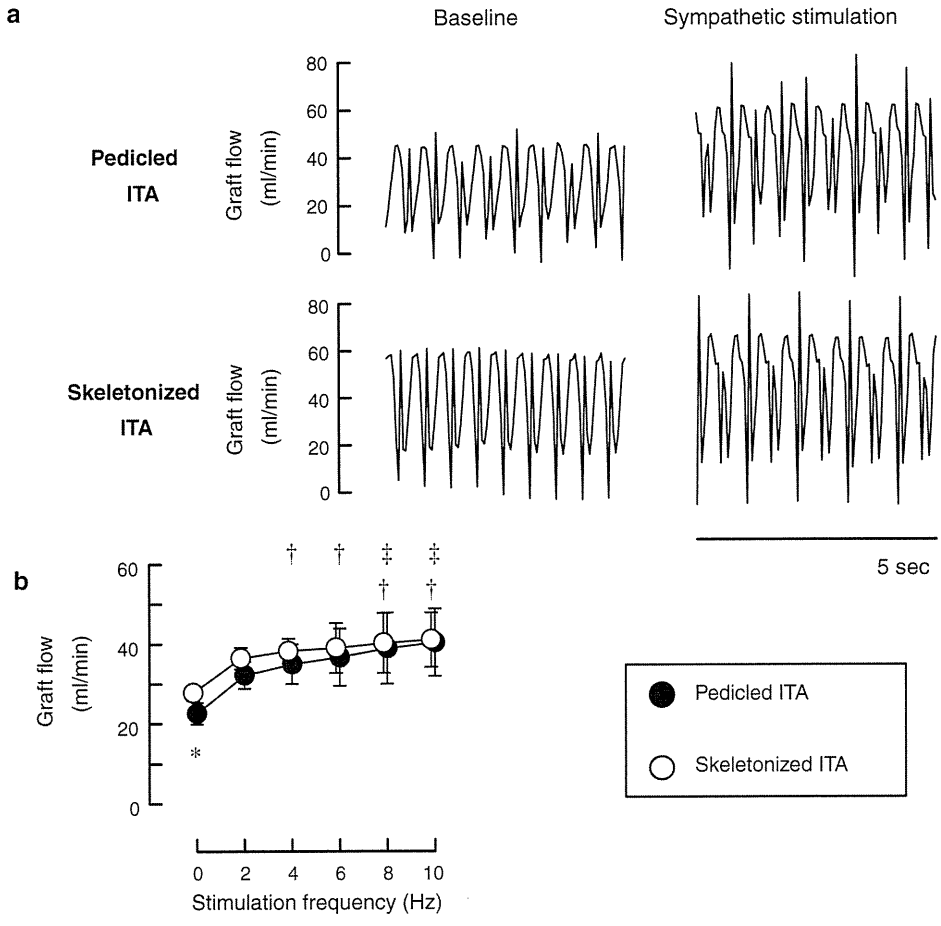

Fig. 1 **a** Typical representative recording of graft flow with pedicled and skeletonized internal thoracic arteries (*ITAs*) during sympathetic nerve stimulation. **b** Mean graft flow with pedicled (*closed circle*) and skeletonized (*open circle*) ITAs during sympathetic nerve stimulation. Data are shown as the mean ± standard error (SE). $^{\dagger}P < 0.05$ vs. baseline, $^{\ddagger}P < 0.01$ vs. baseline, $^{*}P < 0.05$ pedicled vs. skeletonized

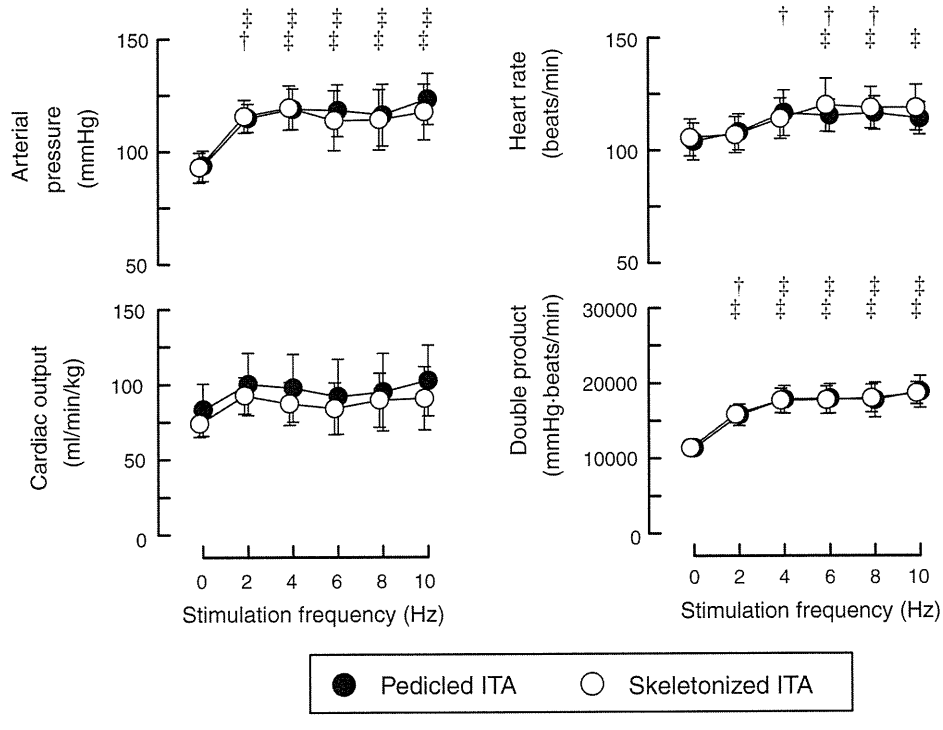

Fig. 2 Changes in mean arterial pressure, cardiac output, heart rate, and double product with pedicled (*closed circle*) and skeletonized (*open circle*) ITAs during sympathetic nerve stimulation. Data are shown as the mean ± SE. $^{\dagger}P < 0.05$ vs. baseline, $^{\ddagger}P < 0.01$ vs. baseline

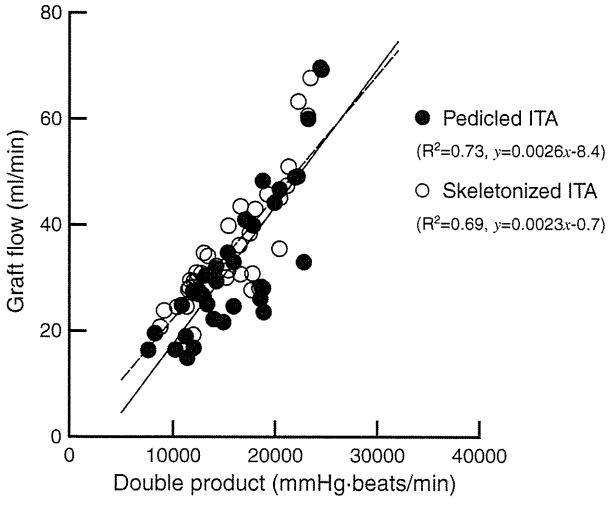

Fig. 3 Scatter plots and regressions between the double product and graft flow with pedicled (*closed circle*, *solid line*) and skeletonized (*open circle*, *dashed line*) ITAs. Regression lines did not differ between the two groups. *y* Graft flow, *x* double product

because the use of contrast medium in angiography may have affected the graft flow through its vasodilatative effect on the coronary artery [11].

Another explanation may be the difference in background sympathetic tone. As the skeletonized graft flow was always studied in the later phase of the experiment, when background sympathetic tone and myocardial metabolic demand may be higher, skeletonized graft flow may have been higher for this reason. The presence of similar hemodynamics during the two protocols, however, does not directly support this explanation. The hemodilution seen predominantly in the later phase of the experiment may also have contributed to higher flow through the skeletonized graft under baseline conditions.

The fact that graft flows were similar between the skeletonized and pedicled ITAs during maximal sympathetic excitation indicates that the resistance of the ITA graft was much smaller than that of the native coronary bed, even when the coronary bed was maximally dilated to meet the oxygen demand present with maximal sympathetic stimulation. In other words, both the skeletonized and pedicled ITAs would appear to provide sufficient flow reserve to the LAD area. In contrast, it has been reported that free flow, which may represent the maximal flow capacity of the ITA itself, is greater in the skeletonized ITA than in the pedicled ITA [2, 3]. Despite these previous findings, because the maximally dilated native coronary bed would be the most practical downstream conduit to test the difference between the skeletonized and pedicled ITAs, we believe that the difference in sympathetic innervation does not affect the maximal flow significantly under anastomosed conditions.

In addition to the effects of downstream resistance, local mechanisms would also contribute to the observed difference in flow between the pedicled and skeletonized ITA grafts. Complete sympathetic denervation with the local application of phenol to the skeletonized ITA further increased graft flow (unpublished observation), suggesting that there remains a certain sympathetic innervation in the skeletonized ITA. Even though sympathetic denervation may not be complete after skeletonization, we believe that our skeletonization did not differ greatly from those clinically performed by surgeons. Deja et al. [4] reported that skeletonization increases the reactivity of ITA to norepinephrine in vitro. Their study may support our results. Prior to sympathetic stimulation but under spontaneous sympathetic outflow, the amount of endogenous norepinephrine release to the skeletonized ITA may be relatively smaller than that to the pedicled ITA; as such, the sympathetic vasoconstriction would be negligible in the skeletonized ITA. This may explain the larger graft flow in the skeletonized ITA prior to sympathetic stimulation. Under maximal sympathetic stimulation, however, hyperreactivity to endogenous norepinephrine in the skeletonized ITA may cause the sympathetic vasoconstriction similar to that occurring in the pedicled ITA. This local mechanism may also partly account for why graft flow was comparable between the pedicled and skeletonized ITAs during maximal sympathetic stimulation. Although the results from several pharmacological studies suggest that norepinephrine-induced vasoconstriction does occur in the ITA [12, 13], there have been no reports assessing the tissue norepinephrine concentration of ITA during sympathetic stimulation. Further investigations are necessary to gain an understanding of the difference in norepinephrine reactivity between the pedicled and skeletonized ITAs.

Some publications have reported several advantages of the skeletonized ITA grafts other than the potential increase in graft flow at rest [1, 14]. Firstly, skeletonization lengthens the ITA, thereby providing access to more distal targets in the coronary artery [15]. Second, skeletonization improves blood supply to the sternum (measured by single photon emission computed tomography) [16] compared with pedicled harvesting. Third, skeletonization decreases the incidence of postoperative respiratory dysfunction because of less invasive harvesting (i.e., preserved pleural integrity in skeletonized ITA vs. pleurotomy in pedicled ITA) [17, 18]. Lastly, skeletonization markedly reduces anterior chest pain and dysesthesia 3 months after surgery [19]. In contrast to these advantages, skeletonization has the minor disadvantages of greater technical difficulty, longer harvesting duration, and potential damage to the graft.

Limitations

This study has several limitations. First, because skeletonized graft flow measurements always follow pedicled graft flow measurements in the same dog, the effect of time sequence on graft flows cannot be ruled out. Nevertheless, the similar hemodynamic response to sympathetic stimulation between protocol 1 and 2 (Fig. 2) suggests that the animal conditions did not deteriorate considerably. Second, the perfusion area of LITA was limited to the LAD region. If we had used a much larger perfusion area of LITA, the possible small difference between the pedicled and skeletonized ITAs may have been revealed. Third, a histological comparison between the pedicled and skeletonized ITA was not performed because the pedicled ITA was always skeletonized after the protocol 1, and the tissue samples from the pedicled ITA could not be obtained. Further investigations that include histological comparison are necessary for examining the effect of skeletonization on sympathetic innervations.

Conclusion

Both the pedicled and skeletonized ITA techniques supplied similar, adequate blood flow to the LAD, meeting myocardial oxygen demand during sympathetic excitation. Metabolic demand can override the possible difference in sympathetic vasoconstriction, increasing the flow in both pedicled and skeletonized ITA grafts to a similar extent when they are anastomosed to LAD. The results of this study have an important implication in terms of clinical application. Following anastomosis, graft flow is highly variable and is dependent on myocardial oxygen demand. Because the quality of CABG may be judged based on flow through anastomosed grafts, one has to take into consideration the potential change in flow in response to myocardial oxygen demand.

Acknowledgments This study was supported by Health and Labor Sciences Research Grants (H18-nano-Ippan-003, H19-nano-Ippan-009, H20-katsudo-Shitei-007 and H21-nano-Ippan-005) from the Ministry of Health, Labor and Welfare of Japan, by Grants-in-Aid for Scientific Research (No. 20390462) from the Ministry of Education, Culture, Sports, Science and Technology in Japan and by the Industrial Technology Research Grant Program from New Energy and Industrial Technology Development Organization (NEDO) of Japan.

References

1. Del Campo C (2003) Pedicled or skeletonized? A review of the internal thoracic artery graft. Tex Heart Inst J 30:170–175
2. Castro GP, Dussin LH, Wender OB, Barbosa GV, Saadi EK (2005) Comparative analysis of the flows of left internal thoracic artery grafts dissected in the pedicled versus skeletonized manner for myocardial revascularization surgery. Arq Bras Cardiol 84:261–266
3. Deja MA, Woś S, Gołba KS, Zurek P, Domaradzki W, Bachowski R, Spyt TJ (1999) Intraoperative and laboratory evaluation of skeletonized versus pedicled internal thoracic artery. Ann Thorac Surg 68:2164–2168
4. Deja MA, Gołba KS, Malinowski M, Woś S, Kolowca M, Biernat J, Kajor M, Spyt TJ (2005) Skeletonization of internal thoracic artery affects its innervation and reactivity. Eur J Cardiothorac Surg 28:551–557
5. Wendler O, Tscholl D, Huang Q, Schäfers HJ (1999) Free flow capacity of skeletonized versus pedicled internal thoracic artery grafts in coronary artery bypass grafts. Eur J Cardiothorac Surg 15:247–250
6. Onorati F, Esposito A, Pezzo F, di Virgilio A, Mastroroberto P, Renzulli A (2007) Hospital outcome analysis after different techniques of left internal mammary grafts harvesting. Ann Thorac Surg 84:1912–1919
7. Takami Y, Ina H (2002) Effects of skeletonization on intraoperative flow and anastomosis diameter of internal thoracic arteries in coronary artery bypass grafting. Ann Thorac Surg 73:1441–1445
8. Austen WG, Edwards JE, Frye RL, Gensini GG, Gott VL, Griffith LS, McGoon DC, Murphy ML, Roe BB (1975) A reporting system on patients evaluated for coronary artery disease. Report of the Ad Hoc Committee for Grading of Coronary Artery Disease, Council on Cardiovascular Surgery, American Heart Association. Circulation 51:5–40
9. Kitamura K, Jorgensen CR, Gobel FL, Taylor HL, Wang Y (1972) Hemodynamic correlates of myocardial oxygen consumption during upright exercise. J Appl Physiol 32:516–522
10. Dönmez A, Tufan H, Tutar N, Araz C, Sezgin A, Karadeli E, Torgay A (2005) In vivo and in vitro effects of stellate ganglion blockade on radial and internal mammary arteries. J Cardiothorac Vasc Anesth 19:729–733
11. Baile EM, Paré PD, D'yachkova Y, Carere RG (1999) Effect of contrast media on coronary vascular resistance: contrast-induced coronary vasodilation. Chest 116:1039–1045
12. Evora PR, Pearson PJ, Discigil B, Oeltjen MR, Schaff HV (2002) Pharmacological studies on internal mammary artery bypass grafts. Action of endogenous and exogenous vasodilators and vasoconstrictors. J Cardiovasc Surg (Torino) 43:761–771
13. He GW, Yang CQ, Starr A (1995) Overview of the nature of vasoconstriction in arterial grafts for coronary operations. Ann Thorac Surg 59:676–683
14. Athanasiou T, Crossman MC, Asimakopoulos G, Cherian A, Weerasinghe A, Glenville B, Casula R (2004) Should the internal thoracic artery be skeletonized? Ann Thorac Surg 77:2238–2246
15. Higami T, Yamashita T, Nohara H, Iwahashi K, Shida T, Ogawa K (2001) Early results of coronary grafting using ultrasonically skeletonized internal thoracic arteries. Ann Thorac Surg 71:1224–1228
16. Cohen AJ, Lockman J, Lorberboym M, Bder O, Cohen N, Medalion B, Schachner A (1999) Assessment of sternal vascularity with single photon emission computed tomography after harvesting of the internal thoracic artery. J Thorac Cardiovasc Surg 118:496–502
17. Bonacchi M, Prifti E, Giunti G, Salica A, Frati G, Sani G (2001) Respiratory dysfunction after coronary artery bypass grafting employing bilateral internal mammary arteries: the influence of intact pleura. Eur J Cardiothorac Surg 19:827–833
18. Matsumoto M, Konishi Y, Miwa S, Minakata K (1997) Effect of different methods of internal thoracic artery harvest on pulmonary function. Ann Thorac Surg 63:653–655

19. Boodhwani M, Lam BK, Nathan HJ, Mesana TG, Ruel M, Zeng W, Sellke FW, Rubens FD (2006) Skeletonized internal thoracic artery harvest reduces pain and dysesthesia and improves sternal perfusion after coronary artery bypass surgery: a randomized, double-blind, within-patient comparison. Circulation 114:766–773

Effect of linear ablation on spectral components of atrial fibrillation

Miki Yokokawa, MD,* Aman Chugh, MD,* Magnus Ulfarsson, PhD,† Hiroshi Takaki, MD, PhD,‡ Li Han, PhD,* Kentaro Yoshida, MD,* Masaru Sugimachi, MD, PhD,‡ Fred Morady, MD, Hakan Oral, MD*

*From the *Division of Cardiovascular Medicine, University of Michigan, Ann Arbor, Michigan, †Department of Electrical and Computer Engineering, University of Iceland, Reykjavik, Iceland, and ‡Department of Cardiovascular Dynamics, National Cardiovascular Center Research Institute, Osaka, Japan.*

BACKGROUND Spectral components of atrial fibrillation (AF) other than the dominant frequency (DF) may represent macroreentrant circuits that coexist with higher-frequency sources during AF.

OBJECTIVE The purpose of this study was to determine whether spectral components of AF can be eliminated by targeted linear ablation.

METHODS Antral pulmonary vein isolation (APVI) and linear ablation were performed in 26 patients (age 60 ± 11 years) to eliminate long-standing persistent AF (duration 3 ± 2 years). Spectral analysis of atrial activation at multiple atrial sites was performed during AF, at baseline, after APVI, and immediately before and after liner ablation along the roof of the left atrium, mitral isthmus, and cavotricuspid isthmus. The prevalence and spatial distribution of spectral components of AF were examined before and after each step of ablation.

RESULTS Twelve (46%) of 26 patients had conversion of AF to atrial tachycardia (AT) during ablation. Mean cycle length of AT was 237 ± 25 ms. A spectral component of AF (3.7 ± 1.2 Hz) other than the DF (6.0 ± 0.9 Hz) was present in 74 (43%) of 173 baseline AF periodograms at multiple atrial sites. Following APVI, no difference in the prevalence of spectral components was seen (38% vs 43%, $P = .38$). However, linear ablation resulted in a significant decrease in the prevalence of spectral components (24% vs 43%, $P < .01$), but only when complete conduction block was achieved.

CONCLUSION Elimination of spectral components of AF by targeted linear ablation suggests that spectral components may indicate site-specific ATs that coexist with AF despite a lower frequency than the DF of AF.

KEYWORDS Atrial fibrillation; Atrial tachycardia; Catheter ablation; Spectral analysis

ABBREVIATIONS **AF** = atrial fibrillation; **APVI** = antral pulmonary vein isolation; **AT** = atrial tachycardia; **CFAE** = complex fractionated atrial electrogram; **CS** = coronary sinus; **DF** = dominant frequency; **LA** = left atrium; **PV** = pulmonary vein; **RA** = right atrium

(Heart Rhythm 2010;7:1732–1737)

A study that analyzed the spectral characteristics of atrial fibrillation (AF) suggested that atrial tachycardias (ATs) to which AF converts during radiofrequency ablation may represent organized tachycardias that coexist with AF despite a lower frequency than the dominant frequency (DF) of AF.[1] If this were the case, targeted linear ablation might eliminate the lower-frequency components.

The purpose of this study was to determine whether linear ablation at sites frequently used by ATs eliminates specific spectral components of AF in patients with persistent AF.

Supported in part by a grant from the Leducq Transatlantic Network.
Address reprint requests and correspondence: Dr. Hakan Oral, Cardiovascular Center, SPC 5853, 1500 East Medical Center Drive, Ann Arbor, Michigan 48109-5853. E-mail address: oralh@umich.edu. (Received May 17, 2010; accepted 2010.)

Methods

Study subjects

The study consisted of 26 patients (23 men and 3 women; mean age 60 ± 11 years, range 35–77 years) with persistent AF who underwent radiofrequency catheter ablation. Mean left atrial (LA) diameter was 46 ± 6 mm, and left ventricular ejection fraction was 0.54 ± 0.09. AF was first diagnosed 8 ± 8 years before presentation and was persistent for 3 ± 2 years before ablation (range 1–7 years). Two patients had coronary artery disease. The clinical characteristics of the patients are listed in Table 1. Patients with a prior ablation procedure were excluded from the study.

Electrophysiologic study

The study protocol was approved by the Institutional Review Board. All patients provided informed written consent. Antiarrhythmic drug therapy was discontinued ≥5 half-lives before electrophysiologic study, except for amiodarone, which was discontinued >8 weeks before the proce-

1547-5271/$ -see front matter doi:10.1016/j.hrthm.2010.05.040

Table 1 Patient characteristics

Age (years)	60 ± 11
Gender (male/female)	19/7
Duration of atrial fibrillation (years)	3 ± 2
Left atrial diameter (mm)	46 ± 6
Left ventricular ejection fraction	0.54 ± 0.09
Coronary artery disease (%)	2 (8)

Values are given as mean ± SD.

dure. Electrophysiologic study was performed in the fasting state under conscious sedation using fentanyl and midazolam. Vascular access was obtained through a femoral vein. A decapolar catheter (E-Z Steer CS Decapolar, Biosense Webster, Diamond Bar, CA, USA) was positioned in the coronary sinus (CS). Immediately after the transseptal puncture, systemic anticoagulation was achieved with intravenous heparin, and the activated clotting time was maintained between 300 and 350 seconds throughout the procedure. The pulmonary veins (PVs) were mapped with a decapolar ring catheter (Lasso, Biosense Webster) advanced to the LA. Mapping and ablation were performed using a 3.5-mm open irrigation tip catheter (ThermoCool NaviStar, Biosense Webster). Bipolar electrograms were displayed and recorded at filter settings of 30 to 500 Hz during the procedure (EPMed Systems, West Berlin, NJ, USA). Electrograms were also recorded at 0.5 to 200 Hz for offline spectral analysis.

Catheter navigation and ablation were performed with guidance from an electroanatomic mapping system (CARTO, Biosense Webster). Radiofrequency energy was delivered at a maximum power of 20 to 25 W at a flow rate of 17 mL/min near the PVs, along the posterior wall, and within the CS and at a maximum power of 35 W at a flow rate of 30 mL/min elsewhere in the atria. Maximum temperature was set at 48°C.

Study protocol and ablation strategy

All patients presented to the laboratory in AF, and ablation was performed during AF. First, antral pulmonary vein isolation (APVI) was performed to isolate all PVs and resulted in termination of AF in 1 of 26 patients. Therefore, the study protocol was completed in the remaining 25 patients who remained in AF after APVI. In these 25 patients, linear ablation along the LA roof and mitral isthmus was performed (Figure 1). At the discretion of the operator, complex fractionated atrial electrograms (CFAEs) were targeted in 20 (80%) of 25 patients. CFAE ablation was performed before linear ablation in 12 (60%) of 20 patients and after liner ablation in 8 (40%) of 20 patients. Linear ablation along the cavotricuspid isthmus was performed in 5 patients who had a history of typical atrial flutter. Whenever AF converted to an AT, entrainment and activation mapping were performed to guide ablation of the AT. Sinus rhythm was restored by transthoracic cardioversion in patients who remained in AF after ablation. After sinus rhythm was restored, conduction block across the LA roof, mitral isthmus, and cavotricuspid isthmus lines was assessed.[2–4] If necessary, additional ablation was performed to achieve complete block.

Prior to ablation, all PVs were mapped with a decapolar ring catheter. Electrograms then were recorded for ≥30 seconds at ≥2 different locations (tagged on the map; Figure 1) at each of the following sites: (1) LA roof, (2) mitral isthmus, (3) LA appendage, (4) LA septum, (5) CS, (6) cavotricuspid isthmus, and (7) right atrial (RA) appendage. Caution was exercised to create linear lesions ≥5 mm from the sampling sites. Sampling was performed at baseline, after APVI, (and also after CFAE ablation when applicable), and immediately before and immediately after linear ablation without any CFAE ablation between the two sampling times.

Digital signal processing and data analysis

Electrograms were processed offline in the MatLab environment (MathWorks, Inc., Natick, MA, USA) using custom software as described previously.[1] In brief, first digitized bipolar electrograms sampled for ≥30 seconds at 2,000 Hz underwent preprocessing steps of bandpass filtering at 40 to 250 Hz, rectification, and low-pass filtering at 20 Hz. Then the discrete Fourier transform of the prepro-

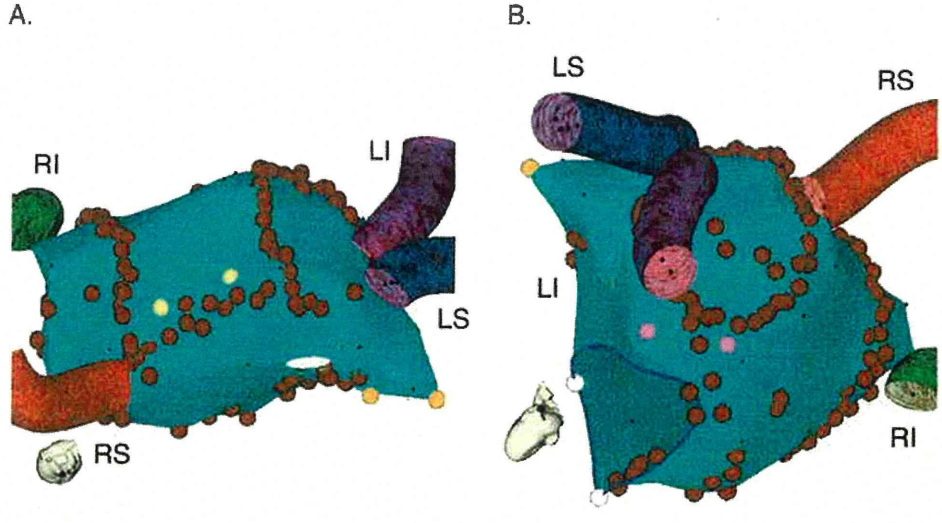

Figure 1 Antral pulmonary vein isolation and linear ablation. Shown is the three-dimensional reconstruction of the left atrium and pulmonary veins during ablation of atrial fibrillation (**A:** craniocaudal projection; **B:** left posterior oblique projection). Electrograms were recorded for ≥30 seconds at ≥2 different positions at each atrial site. *Red tags* indicate ablation sites. *Yellow tags* and *pink tags* indicate sampling sites. LI = left inferior; LS = left superior; RI = right inferior; RS = right superior.

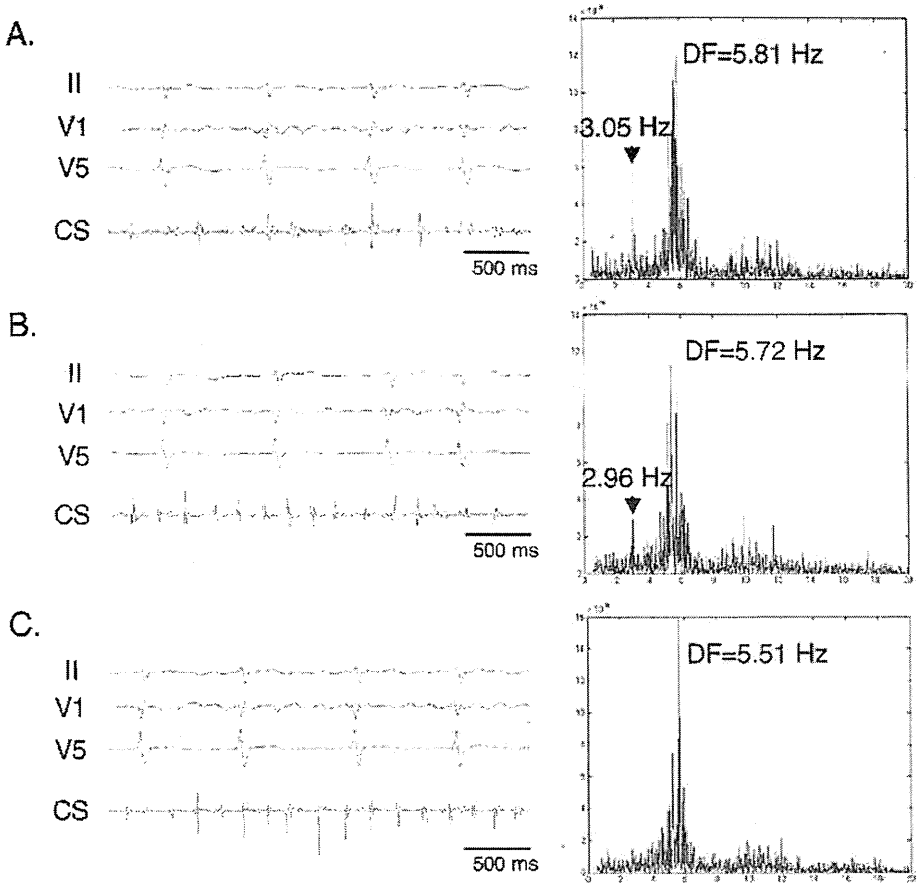

Figure 2 Time- and frequency-domain characteristics of atrial fibrillation (AF) recorded in the coronary sinus (CS). **A:** At baseline, the dominant frequency (DF) of AF was 5.81 Hz, and there was a spectral component with a frequency of 3.05 Hz *(arrow)*. **B:** Antral pulmonary vein isolation (APVI) did not have an effect on the spectral component. **C:** After linear ablation, however, the spectral component was no longer present. Shown are ECG leads II, V_1, and V_5 and bipolar intracardiac electrograms recorded from the CS.

cessed signal was computed using the fast Fourier transformation algorithm to analyze the 0.5- to 80-Hz spectral band. DF was defined as the frequency of the highest peak of the smoothed periodogram in the interval from 0.5 to 20 Hz. The periodogram during AF was systemically analyzed to identify spectral components with peak power ≥20% that of the DF. The spatial distribution of the spectral components of AF and the effect of APVI and linear ablation at specific sites were examined. A site was considered to have a spectral component when a spectral component was identified at any of the sampling sites. When far-field ventricular depolarizations were recorded at the annulus, CS, or appendage, the QRS complexes were subtracted. Electrograms without adequate signal-to-noise ratio were excluded from analysis.

Statistical analysis

Continuous variables, expressed as mean ± SD, were compared using Student's t-test. Sequential continuous variables were compared using one-way analysis of variance with repeated measures. Post hoc comparisons were made with the Scheffe test. Categorical variables were compared using Fisher's exact test. $P < .05$ was considered significant.

Results

DF and spectral components of AF at baseline

At baseline, a spectral component with peak power ≥20% that of the DF was identified at 74 (43%) of 173 sites in 23 of 26 patients (3 ± 2 per patient; Figure 2). The mean frequency of the spectral components was 3.7 ± 1.2 Hz, whereas mean DF at the corresponding sites was 6.0 ± 0.9 Hz ($P < .0001$). There was no significant difference in the spatial distribution of the spectral components among the LA, CS, and RA ($P = .48$; Table 2 and Figure 3).

Antral PV isolation

APVI resulted in complete PV isolation in all patients. AF converted to an AT in 1 (4%) of 26 patients after APVI. APVI resulted in a significant decrease in the DF of AF (5.8 ± 0.9 Hz vs 6.1 ± 0.9 Hz, $P = .03$). There was no significant difference in the prevalence of spectral components before (74/173 sites [43%]) and after APVI (42/112 sites [38%],

Table 2 Effects of APVI and linear ablation on the prevalence of spectral components

	Baseline	After APVI	After linear ablation
All	74/173 (43)	42/112 (38)	27/114 (24)*†
Left atrium	47/104 (45)	24/65 (37)	14/66 (21)*†
Coronary sinus	12/26 (46)	8/19 (42)	4/23 (17)
Right atrium	15/43 (35)	10/28 (36)	9/25 (36)

Percent values are shown in parentheses.
APVI = antral pulmonary vein isolation.
*$P < .01$ compared to baseline; †$P < .05$ compared to immediately before linear ablation.

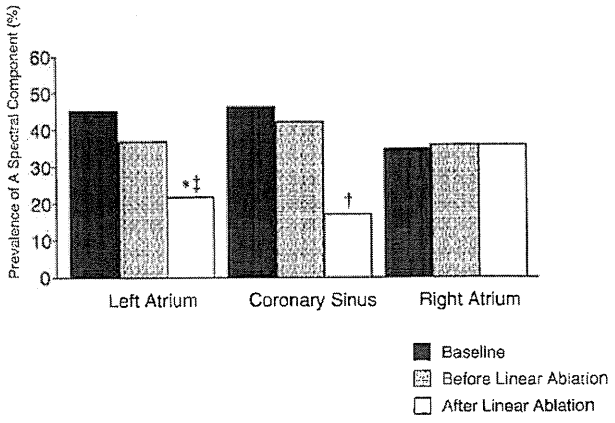

Figure 3 Effect of antral pulmonary vein isolation and linear ablation on the prevalence of spectral components in the left atrium, coronary sinus, and right atrium. *P <.01 and †P = .07 vs compared to baseline; ‡P <.05 compared to immediately before linear ablation.

P = .38; Table 2 and Figure 3). The spatial distribution of the spectral components was also similar before and after APVI (P = .90). There was no significant difference in the mean frequency of the spectral components before and after APVI (3.2 ± 1.2 Hz vs 3.7 ± 1.2 Hz, P = .15).

Ablation of CFAEs did not have a significant effect on the prevalence of spectral components. Among the 12 patients in whom CFAE ablation was performed after APVI but before linear ablation, the prevalence of spectral components was 32% (19/59) after APVI alone and 34% (16/47) after APVI and CFAE ablation (P = .97). Furthermore, the prevalence of spectral components immediately before linear ablation was 34% (16/47) in the 12 patients who had APVI and CFAE ablation before linear ablation and 44% (16/36) in the 8 patients who had CFAE ablation only after linear ablation (P = .33).

Linear ablation

Linear ablation was performed along the LA roof and mitral isthmus in 25 patients and along the cavotricuspid isthmus in 5 patients who remained in AF after APVI. AF converted to an AT in 11 (44%) of 25 patients: after additional linear ablation in 2 patients and after linear and CFAE ablation in 9 patients. Linear ablation was associated with a significant decrease in mean DF in the LA compared to baseline (5.7 ± 0.9 Hz vs 6.1 ± 0.9 Hz, P <.01). There was no significant difference in mean DF after linear ablation compared to the DF after APVI (P = .66). Sinus rhythm was restored by cardioversion in the remaining 14 patients.

Linear ablation resulted in a significant decrease in the prevalence of spectral components with a power ≥20% that of the DF compared to baseline (27/114 sites [24%] vs 74/173 sites [43%], P <.01) and just prior to linear ablation (27/114 sites [24%] vs 42/112 sites [38%], P = .02; Table 2 and Figures 2 and 3). There was a significant decrease in the prevalence of these spectral components after linear ablation at LA sites compared to baseline (14/66 sites [21%] vs 47/104 sites [45%], P <.01) and just prior to linear ablation (14/66 sites [21%] vs 24/65 sites [37%], P <.05). There was a trend toward a decrease in the prevalence of spectral components in the CS (4/23 sites after linear ablation [17%] vs 12/26 sites [46%], P = .07). However, there was no significant change in the prevalence of spectral components at RA sites after linear ablation (9/25 sites [36%] vs 15/43 sites [35%], P = .93).

Linear conduction block and spectral components of AF

Because linear ablation was performed during AF, completeness of conduction block could be assessed only after restoration of sinus rhythm. Complete block was present along the LA roof in 15 (60%) of 25 patients, along the mitral isthmus in 5 (20%) of 25, and along the cavotricuspid isthmus in 2 (40%) of 5 immediately after restoration of sinus rhythm. The spectral components with power ≥20% that of the DF were still present at 12 (55%) of 22 sites with incomplete conduction block and at 0 (0%) of 17 sites with complete conduction block after linear ablation (P <.01). There was no significant change in the mean frequency of spectral components compared to baseline after incomplete linear ablation (3.4 ± 1.0 Hz vs 3.7 ± 1.2 Hz, P = .55).

Prevalence and characteristics of ATs to which AF converts

AF converted to an AT during ablation in 12 (46%) of 26 patients. The mechanism of the ATs was macroreentry in all 12 patients, and their mean cycle length was 237 ± 25 ms (4.3 ± 0.4 Hz). The macroreentrant circuit involved the mitral isthmus in 3 patients, LA roof in 3, interatrial septum in 4, and cavotricuspid isthmus in 2. A spectral component of AF before ablation that matched the frequency of AT was identified at the macroreentrant sites in 6 (50%) of 12 patients (Figure 4). ATs were successfully ablated in all but 4 patients who had pleomorphic ATs. Sinus rhythm was restored by cardioversion in these 4 patients.

DF and termination of AF

At baseline, mean DF was higher among patients who still were in AF after ablation (6.4 ± 0.8 Hz) than among those in whom AF terminated during ablation (5.7 ± 0.9 Hz, P <.0001). Linear ablation was associated with a significant decrease in the DF of AF among patients in whom AF persisted (5.9 ± 0.8 Hz vs 6.4 ± 0.8 Hz, P <.01; Figure 5) and among those in whom AF terminated during ablation (5.3 ± 0.8 Hz vs 5.7 ± 0.9 Hz, P <.01). However, mean DF after linear ablation was still significantly higher when AF persisted than when AF terminated during ablation (5.9 ± 0.8 Hz vs 5.3 ± 0.8 Hz, P <.0001), particularly in the LA appendage (6.1 ± 0.7 Hz vs 5.2 ± 0.9 Hz, P <.01).

Prevalence of spectral components and termination of AF

The prevalence of spectral components of AF at baseline was significantly higher among patients in whom AF persisted than in those in whom AF terminated during ablation

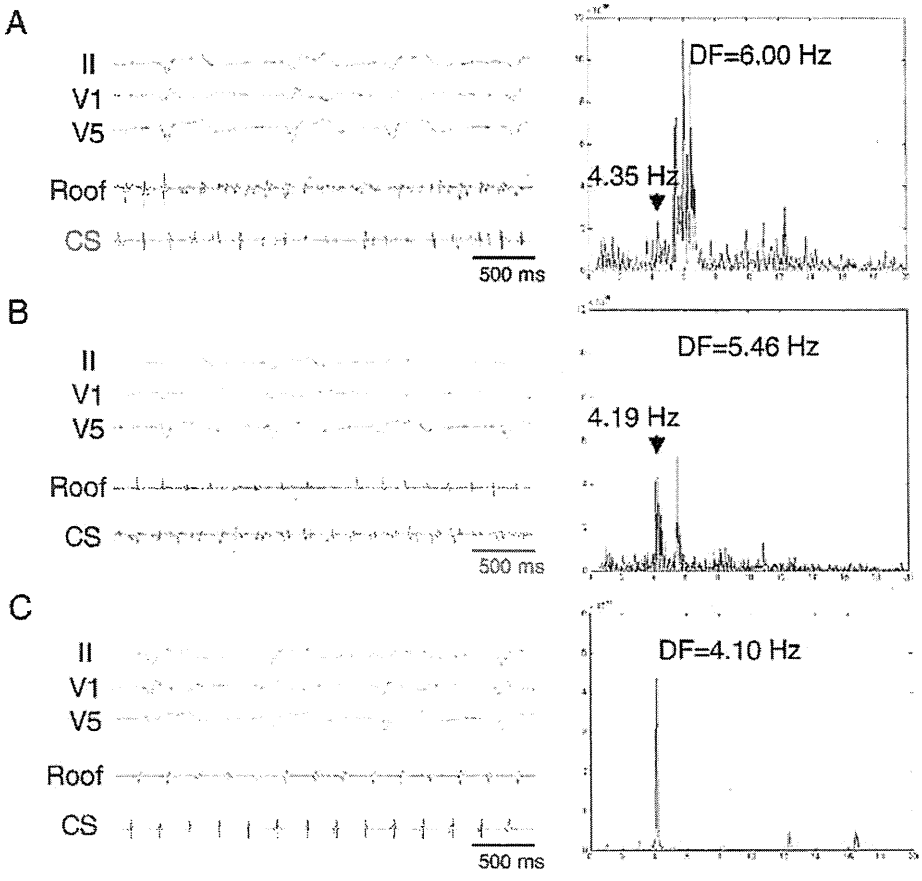

Figure 4 Time- and frequency-domain characteristics of atrial fibrillation (AF) recorded at the left atrial (LA) roof. **A:** At baseline, a spectral component with a frequency of 4.35 Hz was identified *(arrow)*. The simultaneous dominant frequency (DF) was 6 Hz. During linear ablation, AF first became more organized (**B**), then converted to an atrial tachycardia (**C**). The frequency of the spectral component during AF at baseline (**A**) and the atrial tachycardia to which AF converted during ablation (**C**) was similar. The flutter circuit used the LA roof and was successfully ablated with a roof line. Shown are ECG leads II, V_1, and V_5 and bipolar intracardiac electrograms recorded from the LA roof and coronary sinus (CS).

(53/92 sites [58%] vs 21/81 sites [26%], P <.0001). At baseline, the mean frequency of spectral components was 3.7 ± 1.3 Hz when AF persisted and 3.8 ± 0.9 Hz when AF terminated during ablation (P = .79).

Discussion

Major findings

The main findings of this study were as follows. (1) A spectral component with power ≥20% that of the DF was present in 43% of baseline periodograms in patients with persistent AF. (2) Linear ablation, but not APVI, resulted in a significant decrease in the prevalence of these spectral components when complete conduction block was achieved. (3) Spectral components were more prevalent at baseline among patients in whom AF persisted than in those in whom AF terminated during ablation.

Taken together, these findings suggest that spectral components other than the DF may reflect site-specific tachycardias that coexist with AF and can be eliminated by targeted linear ablation. Spectral components of AF appear to reflect contributors of AF perpetuation.

Spectral components of AF

As suggested in a prior study,[1] spectral components of AF may indicate ATs that coexist with AF and that are uncovered after elimination of higher-frequency drivers and fibrillatory conduction by ablation. Because the frequency of the spectral components often matches the frequency of ATs to which AF converts during ablation and because these ATs frequently are macroreentrant circuits that use the roof and mitral isthmus, this study investigated the effects of linear ablation on spectral components.

APVI did not affect the prevalence and frequency of spectral components. CFAE ablation was also performed before (60%) or after linear ablation (40%) in a majority of patients in this study. Similar to APVI, ablation of CFAEs did not have a significant effect on the prevalence of spectral components. However, complete conduction block after linear ablation at these sites led to a significant decrease in the prevalence of spectral components, with no change when conduction block was incomplete. This finding suggests that the spectral components represent underlying macroreentrant circuits eliminated by linear ablation and not simply passive bystander activation or fibrillatory conduction. Furthermore, LA linear ablation had an effect only on the LA spectral components. There was no change in the prevalence of RA spectral components.

An important observation is that APVI resulted in a significant decrease in the DF of AF but had no effect on the frequency of spectral components. Therefore, spectral components likely are not due to passive activation from high-frequency drivers of AF, such as PV tachycardias. If spec-

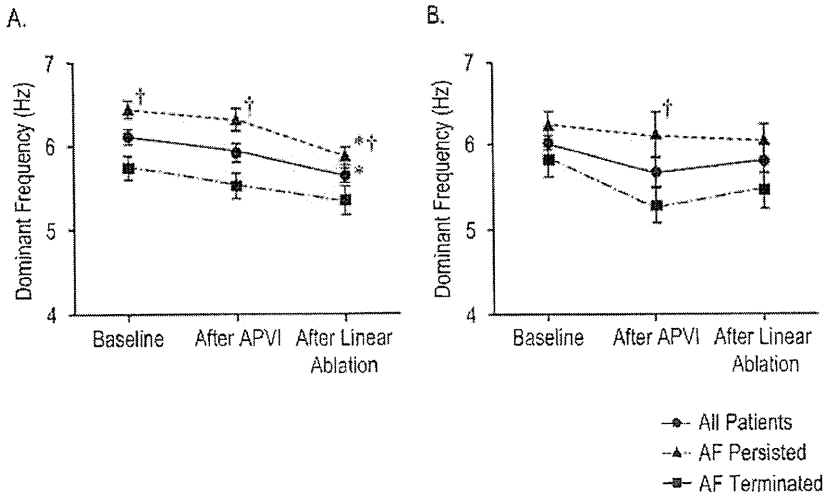

Figure 5 Effect of antral pulmonary vein isolation (APVI) and linear ablation on the dominant frequency of atrial fibrillation (AF) recorded in the left atrium (A) and right atrium (B) among patients who did and those who did not have termination of AF after ablation. *P <.01 compared to baseline; †P <.01 among patients who did and those who did not have termination of AF after ablation.

tral components were secondary due to passive activation, a decrease in the DF of AF should have to led to a decrease in the frequency of the spectral components.

Spectral components and termination of AF

Spectral components were more prevalent among patients in whom AF persisted than among those in whom AF terminated during ablation in this study. Because it can be speculated that spectral components represent underlying drivers of AF masked by fibrillatory conduction, a higher prevalence of spectral components may indicate a larger number of contributors to perpetuation of AF and a higher degree of complexity.

This observation suggests that elimination of a few drivers with the highest frequency often may not be sufficient for termination of AF during ablation. The presence and multiplicity of drivers with a lower frequency than the DF of AF may also be important in perpetuating AF.

A prior study demonstrated that linear ablation is necessary to terminate AF in approximately 90% of patients with long-standing persistent AF.[5] Because the roof, mitral isthmus, and cavotricuspid isthmus seldom are the sites with the highest frequency, it is possible that linear ablation exerts its beneficial effect by eliminating underlying secondary or slower drivers of AF.[6] It also is possible that fibrillatory conduction develops out of macroreentrant circuits represented by spectral components during AF.[7]

Study limitations

One limitation of this study is that the prevalence of spectral components may have been underestimated because simultaneous high-density mapping of the LA was not performed. A second limitation is that, due to the effects of ablation and the signal-to-noise ratio, some of the matching electrograms before and after ablation could not be analyzed. However, a sufficient number of electrograms were available for analysis, and the distribution of poor-quality electrograms was random among different sites. Furthermore, there was no difference in the prevalence of spectral components at baseline among sites where samples after linear ablation were and were not available. A third limitation is that because RA ablation was limited to the cavotricuspid isthmus and was performed in only five patients, the effect of RA ablation on prevalence of RA spectral components may have been underestimated.

Clinical implications

The findings of this study suggest that spectral components of AF other than DF may represent underlying ATs likely to play a role in the perpetuation of AF. The ATs that coexist with AF can be eliminated by targeted linear ablation, but only when complete conduction block is achieved, underscoring the importance of assessing conduction block once sinus rhythm has been restored.

Whether spectral components can be identified in real time and used to guide linear ablation during catheter ablation of AF remains to be determined in future studies.

References

1. Yoshida K, Chugh A, Ulfarsson M, et al. Relationship between the spectral characteristics of atrial fibrillation and atrial tachycardias that occur after catheter ablation of atrial fibrillation. Heart Rhythm 2009;6:11–17.
2. Hocini M, Jais P, Sanders P, et al. Techniques, evaluation, and consequences of linear block at the left atrial roof in paroxysmal atrial fibrillation: a prospective randomized study. Circulation 2005;112:3688–3696.
3. Jais P, Hocini M, Hsu LF, et al. Technique and results of linear ablation at the mitral isthmus. Circulation 2004;110:2996–3002.
4. Chugh A, Oral H, Good E, et al. Catheter ablation of atypical atrial flutter and atrial tachycardia within the coronary sinus after left atrial ablation for atrial fibrillation. J Am Coll Cardiol 2005;46:83–91.
5. Haissaguerre M, Hocini M, Sanders P, et al. Catheter ablation of long-lasting persistent atrial fibrillation: clinical outcome and mechanisms of subsequent arrhythmias. J Cardiovasc Electrophysiol 2005;16:1138–1147.
6. Sanders P, Berenfeld O, Hocini M, et al. Spectral analysis identifies sites of high-frequency activity maintaining atrial fibrillation in humans. Circulation 2005;112:789–797.
7. Sahadevan J, Ryu K, Peltz L, et al. Epicardial mapping of chronic atrial fibrillation in patients: preliminary observations. Circulation 2004;110:3293–3299.